MCB
Journals.ASM.org

Transthyretin Blocks Retinol Uptake and Cell Signaling by the Holo-Retinol-Binding Protein Receptor STRA6

Daniel C. Berry,[a,b] Colleen M. Croniger,[b] Norbert B. Ghyselinck,[c] and Noa Noy[a,b]

Departments of Pharmacology[a] and Nutrition,[b] Case Western Reserve University School of Medicine, Cleveland, Ohio, USA, and Institut de Génétique et de Biologie Moléculaire et Cellulaire, Centre National de la Recherche Scientifique (UMR7104), Institut National de la Santé et de la Recherche Médicale U964, Université de Strasbourg, Illkirch, France[c]

Vitamin A is secreted from cellular stores and circulates in blood bound to retinol-binding protein (RBP). In turn, holo-RBP associates in plasma with transthyretin (TTR) to form a ternary RBP-retinol-TTR complex. It is believed that binding to TTR prevents the loss of RBP by filtration in the kidney. At target cells, holo-RBP is recognized by STRA6, a plasma membrane protein that serves a dual role: it mediates uptake of retinol from extracellular RBP into cells, and it functions as a cytokine receptor that, upon binding holo-RBP, triggers a JAK/STAT signaling cascade. We previously showed that STRA6-mediated signaling underlies the ability of RBP to induce insulin resistance. However, the role that TTR, the binding partner of holo-RBP in blood, plays in STRA6-mediated activities remained unknown. Here we show that TTR blocks the ability of holo-RBP to associate with STRA6 and thereby effectively suppresses both STRA6-mediated retinol uptake and STRA6-initiated cell signaling. Consequently, TTR protects mice from RBP-induced insulin resistance, reflected by reduced phosphorylation of insulin receptor and glucose tolerance tests. The data indicate that STRA6 functions only under circumstances where the plasma RBP level exceeds that of TTR and demonstrate that, in addition to preventing the loss of RBP, TTR plays a central role in regulating holo-RBP/STRA6 signaling.

Vitamin A (retinol [ROH]) plays critical roles both in the embryo and in the adult, where it regulates multiple cellular processes and is essential for embryonic development, reproduction, immune function, and vision (29, 32, 33). The vitamin exerts many of its biological activities by giving rise to active metabolites: the visual chromophore 11-*cis*-retinaldehyde and retinoic acid (RA), which regulates gene transcription by activating specific nuclear receptors (11, 27). ROH is stored in various tissues, including white adipose tissue (WAT), lung, and retinal pigment epithelium in the eye, but its main storage site is the liver. ROH is secreted from storage into the circulation bound to retinol-binding protein (RBP), a 21-kDa polypeptide that contains one binding site for ROH. In most mammals, ROH-bound RBP (holo-RBP) does not circulate alone but is associated with another protein called transthyretin (TTR), a 56-kDa homotetramer that, in addition to associating with RBP, functions as a carrier for thyroid hormones (23, 24). ROH thus reaches target tissues bound in a holo-RBP-TTR complex that, under normal circumstances, displays a 1:1 molar stoichiometry. It is believed that binding of RBP to TTR serves to prevent the loss of the smaller protein from blood by filtration in the glomeruli. The concentration of the holo-RBP-TTR complex in plasma is kept constant at 1 to 2 μM except in extreme cases of vitamin A deficiency or in disease states. Notably, RBP levels are markedly elevated in blood of obese mice and humans, and it was reported that, under these circumstances, the protein induces insulin resistance (35).

Association with the TTR-RBP complex allows the poorly soluble ROH to circulate in blood, but the vitamin dissociates from RBP prior to entering cells. It was proposed that, due to its hydrophobic nature, ROH can readily move from extracellular RBP into cells by diffusion across the plasma membranes at fluxes that are dictated by its extracellular-to-intracellular concentration gradient (10, 14, 20, 21). However, it has also been suggested that uptake of ROH from circulating holo-RBP is mediated by a cell surface receptor (13, 28). Indeed, a plasma membrane protein termed STRA6 (stimulated by retinoic acid 6) was found to bind holo-RBP and transport ROH into cells (15). Our recent studies revealed that, in addition to its function as an ROH transporter, STRA6 is a cytokine receptor. We thus found that binding of holo-RBP triggers phosphorylation of a tyrosine residue in the cytosolic domain of STRA6, resulting in recruitment and activation of the Janus kinase JAK2 and, in a cell-dependent manner, the transcription factors STAT3 or STAT5. Holo-RBP thus activates STRA6-mediated signaling that culminates in upregulation of STAT target genes (2, 4). As STAT target genes in white adipose tissue and muscle include *Suppressor of cytokine signaling 3* (*Socs3*), a potent inhibitor of insulin signaling (8), these findings suggested a rationale for understanding how elevated serum levels of RBP in obese animals induce insulin resistance (35). Additional studies showed that activation of STRA6 is triggered not simply by binding of holo-RBP but by a STRA6-mediated translocation of ROH from extracellular holo-RBP to an intracellular acceptor, the retinol-binding protein CRBP-I. Importantly, this movement was found to be critically linked to the intracellular metabolism of ROH (5). The data further established that ROH uptake and signaling by STRA6 are interdependent, i.e., that activation of a JAK2/STAT cascade by the receptor requires ROH uptake and, conversely, that phosphorylation of STRA6 is essential for enabling ROH transport to proceed (5).

Received 8 June 2012 Returned for modification 8 July 2012
Accepted 15 July 2012
Published ahead of print 23 July 2012
Address correspondence to Noa Noy, noa.noy@case.edu.

doi:10.1128/MCB.00775-12

While these recent studies provided surprising new insights into the involvement of STRA6 in vitamin A biology, the role that TTR, the binding partner of holo-RBP in blood, may play in STRA6-mediated functions remained unknown. Here, we show that TTR blocks the ability of holo-RBP to associate with STRA6 and thereby effectively suppresses both STRA6-mediated ROH uptake and STRA6-initiated cell signaling. We show further that, consequently, TTR protects mice from RBP-induced insulin resistance. The data indicate that, in addition to preventing the loss of RBP by filtration in the kidney, TTR plays a central role in regulating holo-RBP/STRA6 signaling.

MATERIALS AND METHODS

Reagents. Human STRA6 was cloned as an N-terminal six-histidine-tagged protein in a pReceiver-M01 vector (GeneCopoeia). Point mutations of RBP were generated using the Stratagene Quikchange II mutagenesis kit. Lentiviruses harboring small hairpin RNA (shRNA) for STRA6 were purchased from Openbiosystems. Antibodies against actin and six-histidine were from Santa Cruz Biotechnology. Antibodies against JAK2, pJAK2, pAKT, pIR, IR, pSTAT5, STAT5, and phosphotyrosine were from Cell Signaling. RBP antibodies were purchased from Dako. Retinol and bovine insulin were purchased from Sigma Chemical Co., and retinol was purchased from Calbiochem.

Immunoblots and immunoprecipitations were performed as previously described (2).

Mouse studies. Mice with a mixed C57BL/6-129/Sv (50%-50%) genetic background were maintained on a 12-h light and dark cycle on a normal chow diet. Mice were housed according to the Animal Resource Center (ARC) protocol. The breeding diets (diet no. 5P76 from LabDiet) contained 25,000 to 29,000 IU of vitamin A per kg. The mice had access to water and diet *ad libitum*.

Cells. HepG2 and NIH 3T3 cells were cultured in Dulbecco's modified Eagle medium (DMEM) supplemented with 10% fetal bovine serum (FBS) and 10% calf serum, respectively. NIH 3T3-L1 preadipocytes were induced to differentiate, and differentiation was verified as previously described (3).

Analysis of mRNA. RNA was extracted using TRIzol (Molecular Research Center). cDNA was generated using GeneAmp RNA PCR (Applied Biosystems). Quantitative PCR (Q-PCR) was carried out using TaqMan chemistry and Assays-on-Demand probes (Applied Biosystems) for hSTRA6 (Hs00223621_m1), hSOCS3 (Hs02330328_g1), mSOCS3 (Mm01249143), mPPARγ (Mm00440945_m1), and 18s rRNA (4352930). RNA was extracted from lipid tissues and skeletal muscle using the RNeasy lipid tissue minikit (Qiagen catalog no. 74804) and RNeasy fibrous tissue minikit (catalog no. 74704).

Recombinant proteins. Bacterial expression vectors for histidine-tagged hRBP and hTTR were respectively provided by Lawreen Connors, Boston University School of Medicine, and Silke Vogel, Columbia University. RBP and TTR were expressed in *Escherichia coli* and purified as previously described (see reference 34 for RBP and reference 16 for TTR). Purified proteins were dialyzed against 300 mM NaCl, 100 mM Tris (pH 7.4), and 5% glycerol. For RBP, the method generates holo-RBP, i.e., an RBP-ROH complex at a 1:1 molar ratio.

Vitamin A uptake by cultured cells. Holo-RBP was incubated with [^{3}H]retinol (~5,000 cpm/nmol) for 2 h on ice. In experiments including TTR, ^{3}H-labeled holo-RBP was precomplexed with TTR prior to experimentation. Cultured cells were placed in serum-free media for 12 h prior to experimentation. Cells were then washed three times with phosphate-buffered saline (PBS), placed in serum-free media, and treated with 1 μM [^{3}H]RBP-ROH or [^{3}H]RBP-ROH-TTR for 3 min. Cells were washed twice with PBS and then placed in 100% ethanol for 10 min. The ethanol phase was immediately quantified using a scintillation counter (Beckman Coulter LS6500). The protein content of each well was measured using the Bradford assay and used for data normalization.

Uptake of ROH from holo-RBP *in vivo*. Mice fed a regular chow diet were intraperitoneally injected with 0.2 mg holo-RBP or holo-RBP-TTR containing 0.02 mCi [^{3}H]ROH-RBP (total volume, 60 μl). Two hours postinjection, a blood sample was collected, and hearts were perfused with 0.9% saline to remove blood containing labeled ROH. Tissues were isolated, weighed, and stored in liquid nitrogen. Tissues were homogenized in PBS, and homogenates were placed in scintillation fluid and counted (Beckman Coulter). Counts were normalized per gram tissue.

GTT. For glucose tolerance tests (GTT), mice were fasted for 12 h and injected intraperitoneally with glucose (2 g kg^{-1} of body weight). Blood was sampled from the tail vein at 0, 15, 30, 60, and 120 min using an UltraTouch or Accu-Chek Performa glucometer.

Fluorescence titrations. Binding of ROH to RBP or its mutant was monitored by fluorescence titrations as described previously (7). Prior to titrations, ROH was extracted from purified holo-RBP as described previously (7). Ligand binding was monitored by following the increase in ROH fluorescence (excitation wavelength [λ_{ex}] = 325 nm; emission wavelength [λ_{em}] = 480 nm) that accompanies binding to the protein. Titration curves were analyzed by fitting the data to an equation derived from simple binding theory (19) using the software Origin (MicroCal).

Fluorescence anisotropy titrations. The association between holo-RBP and TTR was monitored by following the increase in fluorescence anisotropy of RBP-bound ROH (λ_{ex} = 325; λ_{em} = 480 nm) that accompanies complex formation. Measurements were carried out using a Photon Technology International Quantamaster spectrofluorometer equipped with Glan-Thompson polarizers.

RESULTS

TTR inhibits STRA6-mediated uptake of ROH from holo-RBP. In most mammals, holo-RBP circulates in blood in complex with transthyretin (TTR). To begin to examine the effect of TTR on STRA6 function, hepatocarcinoma HepG2 cells, which endogenously express STRA6, were used to compare the cellular uptake of ROH from holo-RBP and from TTR-bound holo-RBP. Recombinant RBP and TTR were expressed in *E. coli* and purified (see Materials and Methods). HepG2 cells were treated with RBP complexed with [^{3}H]retinol at a 1 μM concentration, similar to the serum RBP level, or with 1 μM [^{3}H]retinol-labeled RBP complexed with TTR at a 1:1 molar stoichiometry, similar to that found in blood (24). Media were removed, cells washed, and organic compounds extracted from the cells into ethanol, and the amount of [^{3}H]retinol taken up within the incubation period was measured by scintillation counting. The rates of uptake of retinol under the assay conditions were constant during the initial 5 min (Fig. 1a), and subsequent experiments were carried out with a single 3-min time point, well within the initial linear rate. The rate of ROH uptake from the holo-RBP-TTR complex was lower than that of the uptake from holo-RBP alone (Fig. 1a). Moreover, increasing the TTR/RBP ratio by increasing the concentration of TTR inhibited ROH uptake in a dose-dependent manner (Fig. 1b). The dose response of the initial rate of ROH transport from holo-RBP showed a two-phase behavior comprised of an initial saturable component, likely attributable to STRA6-mediated uptake, followed by a nonsaturable phase, reflecting passive diffusion of ROH across the plasma membranes (Fig. 1c). In contrast, uptake of ROH from the holo-RBP-TTR complex displayed a single, nonsaturable phase (Fig. 1c). These observations suggest that TTR does not impede the ability of ROH to enter cells by passive diffusion but effectively blocks ROH transport mediated by STRA6. In agreement with this notion, increasing the expression level of STRA6 in HepG2 cells (Fig. 1d) facilitated ROH uptake from holo-RBP in a dose-responsive manner but had no ef-

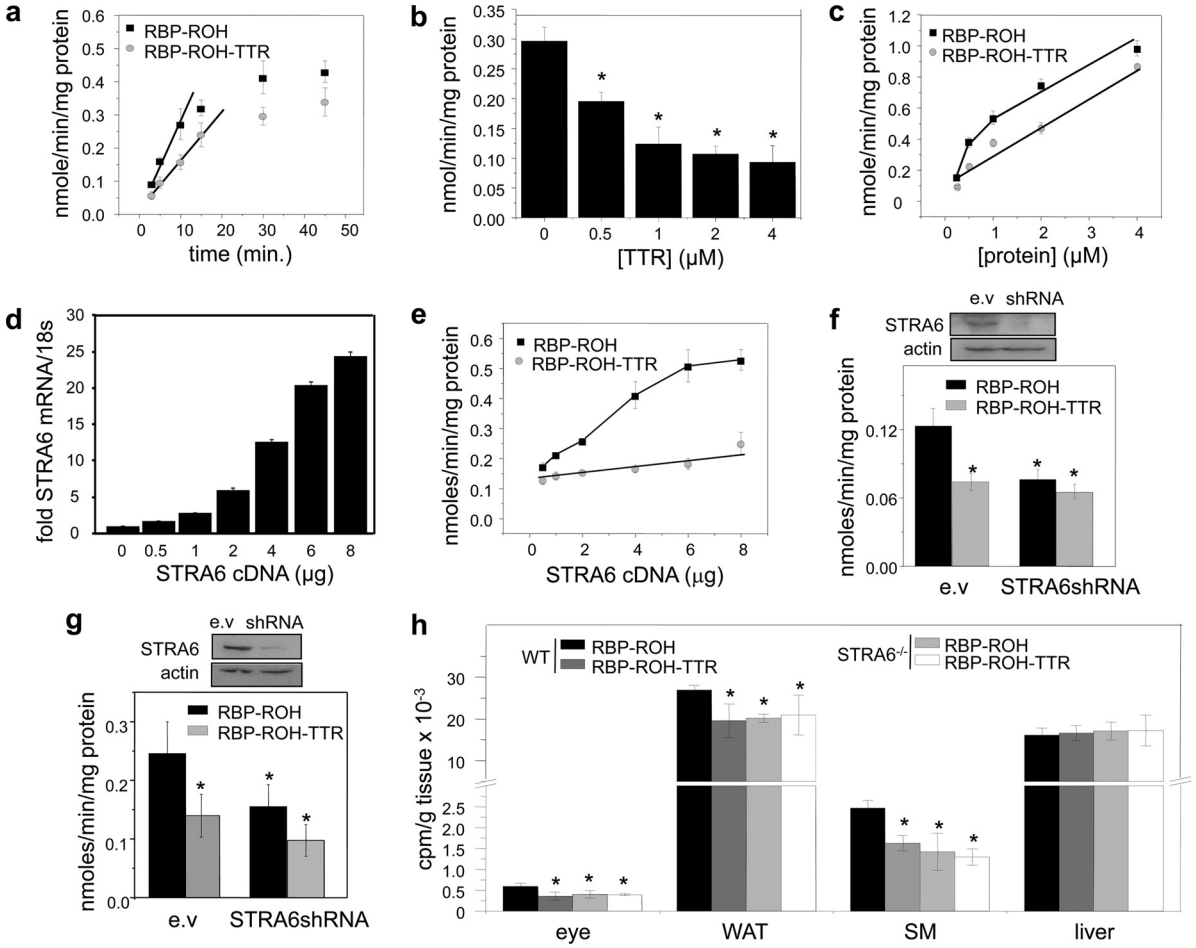

FIG 1 TTR inhibits STRA6-mediated uptake of ROH from holo-RBP. (a) Uptake of [^{3}H]ROH by HepG2 cells treated with RBP-[^{3}H]ROH or RBP-[^{3}H]ROH-TTR (1 μM) for denoted times. (b) Uptake of [^{3}H]ROH by HepG2 cells treated with the denoted concentrations of RBP-[^{3}H]ROH or RBP-[^{3}H]ROH-TTR for 3 min. (c) Uptake of [^{3}H]ROH by HepG2 cells following a 3-min incubation with 1 μM RBP-[^{3}H]ROH in the presence of denoted concentrations of TTR. (d) Levels of STRA6 mRNA in HepG2 cells transfected with various amounts of STRA6 cDNA. (e) Effect of increasing the expression level of STRA6 in HepG2 cells on uptake of [^{3}H]ROH from RBP-[^{3}H]ROH or RBP-[^{3}H]ROH-TTR (1 μM, 3 min). (f) Top, expression level of STRA6 in HepG2 cells transfected with an empty vector (e.v.) or vector harboring STRA6shRNA. Bottom, effect of decreasing the expression level of STRA6 in HepG2 cells on uptake of [^{3}H]ROH from RBP-[^{3}H]ROH or from RBP-[^{3}H]ROH-TTR (1 μM, 3 min). (g) Top, expression level of STRA6 in NIH 3T3-L1 cells transfected with an empty vector (e.v.) or a vector harboring STRA6shRNA. Bottom, effect of decreasing the expression level of STRA6 in NIH 3T3-L1 adipocytes on uptake of [^{3}H]ROH from RBP-[^{3}H]ROH or from RBP-[^{3}H]ROH-TTR (1 μM, 3 min). (h) Twelve-week-old WT and STRA6-null male mice were injected intraperitoneally with RBP-[^{3}H]ROH (100 μl, 0.1 mCi, 1 μM). Two hours later, tissues were isolated, weighed, and homogenized, and [^{3}H]ROH was quantified. Data are means ± standard errors of the means; *, $P < 0.01$ for RBP-ROH-treated versus RBP-ROH-TTR-treated groups. All *P* values were calculated using a two-tailed Student *t* test.

fect on transport of ROH from TTR-bound holo-RBP (Fig. 1e). Also in agreement, decreasing the expression of STRA6 in HepG2 cells (Fig. 1f) or in NIH 3T3-L1 adipocytes (Fig. 1g) reduced the rate of ROH uptake from holo-RBP but did not affect uptake from TTR-bound holo-RBP. The observation that, in both cell lines, rates of uptake from the holo-RBP-TTR complex were similar to those observed in the absence of STRA6 supports the conclusion that TTR specifically inhibits STRA6-mediated transport.

The effect of TTR on ROH uptake from holo-RBP was then examined *in vivo* using our newly generated STRA6-null mice (26). Twelve-week-old wild-type (WT) and STRA6-null male mice were injected intraperitoneally with [^{3}H]ROH-labeled holo-RBP or with holo-RBP complexed with TTR, and ROH uptake into tissues was assessed 2 h later. Uptake of ROH into the STRA6-expressing tissues WAT, skeletal muscle, and the eye was modestly but significantly lower in STRA6-null than in WT mice (Fig. 1h), reflecting that the contribution of STRA6 to overall vitamin A uptake by tissues *in vivo* is small. ROH uptake from TTR-bound holo-RBP was all but identical to that observed in STRA6$^{-/-}$ animals (Fig. 1h). Neither ablation of STRA6 nor the presence of TTR affected ROH uptake by the liver, an organ that does not express STRA6 (Fig. 1h). Hence, TTR specifically inhibits STRA6-mediated uptake of ROH *in vivo*.

TTR inhibits the association of holo-RBP with STRA6. STRA6 may bind the ternary RBP-ROH-TTR complex or, alternatively, it may recognize only free holo-RBP. To dissect these possibilities, we considered that, unlike in most mammals, holo-RBP in zebrafish (*Danio rerio*) does not associate with TTR. Thus, presumably, zebrafish STRA6 does not contain a TTR-binding region, and while ROH uptake by the mammalian STRA6 may involve recognition of TTR, ROH uptake by zebrafish STRA6 (dSTRA6) will not. In these experiments, NIH 3T3 fibroblasts,

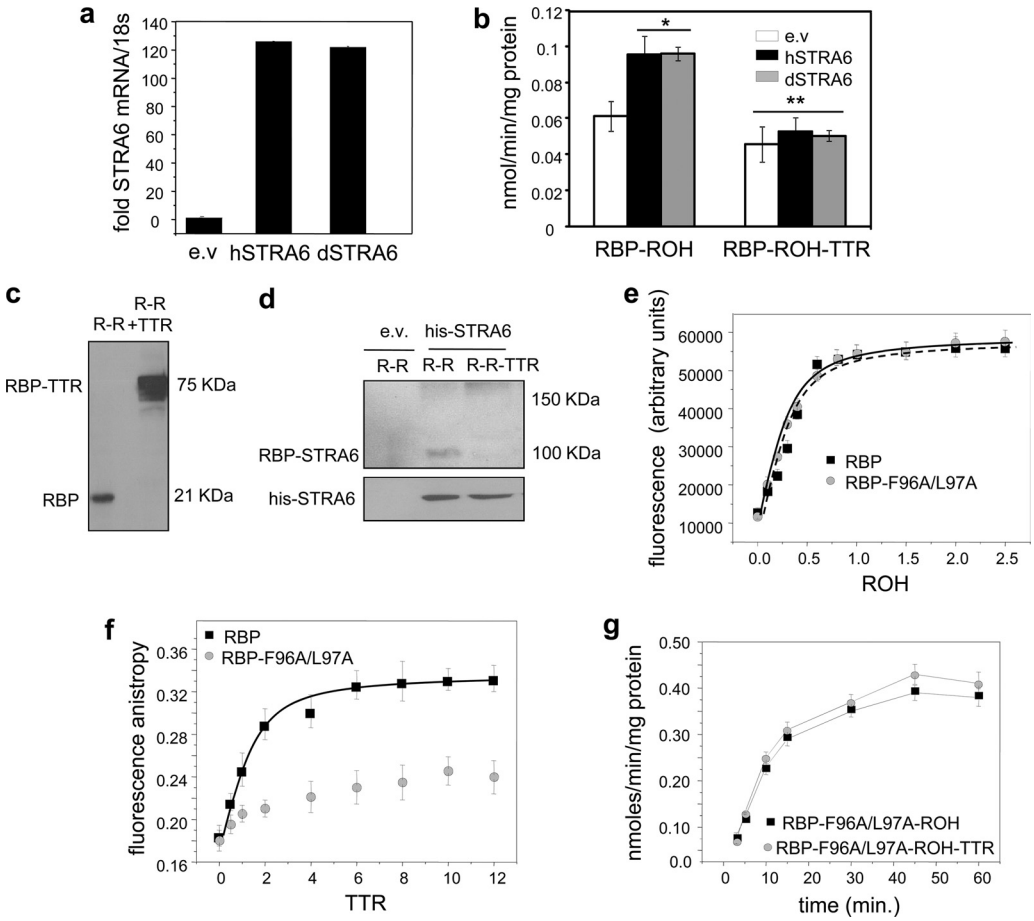

FIG 2 STRA6 does not bind the holo-RBP-TTR complex. (a) NIH 3T3 cells stably overexpressing LRAT were transfected with an empty vector (e.v.) or with expression vectors encoding human (hSTRA6) or zebrafish (dSTRA6) STRA6, resulting in similar levels of mRNAs. (b) Uptake of [^{3}H]ROH from RBP-[^{3}H]ROH or RBP-[^{3}H]ROH-TTR (1 μM, 3 min) by cells expressing hSTRA6 or dSTRA6. (c) RBP-ROH (R-R) or RBP-ROH-TTR (R-R + TTR) (1 μM) was incubated with the chemical cross-linker bis(sulfosuccinimidyl) suberate (0.5 mM) for 14 h. Proteins were resolved by SDS-PAGE and visualized by Coomassie blue staining. (d) Cross-linked complexes and additional cross-linker (0.5 mM) were added to HepG2 cells transfected with an e.v. or with a vector encoding histidine-tagged STRA6. Following a 15-min incubation, his-STRA6 was immunoprecipitated using antibodies against the tag, and precipitated RBP and STRA6 were visualized by immunoblotting. (e) Fluorescence titrations of RBP and its F96A/L97A mutant (1 μM) with ROH. Progress of titrations was monitored by following the increase in ROH fluorescence upon binding to the protein (λ_{ex} = 330 nm; λ_{em} = 460 nm). (f) Fluorescence anisotropy titrations of holo-RBP and holo-RBP-F96A/L97A (3 μM) with TTR. Progress of titrations was monitored by measuring the fluorescence anisotropy of bound ROH (λ_{ex} = 330 nm; λ_{em} = 460 nm). (g) Uptake of [^{3}H]ROH from holo-RBP-F96A/L97A (1 μM, 3 min) in the presence or absence of TTR. Data are means ± standard errors of the means (SEM). *, $P < 0.01$ versus cells transfected with an empty vector; **, $P = 0.01$ versus cells transfected with an empty vector and treated with RBP-ROH. All P values were calculated using a two-tailed Student t test.

which do not endogenously express STRA6, were used. We previously showed that ROH metabolism is essential both for STRA6-mediated ROH transport and for holo-RBP-induced STRA6 signaling (5). Hence, to enable STRA6 action in these cells, an NIH 3T3 line in which ROH metabolism is enhanced by stably overexpressing lecithin:ROH-acyltransferase (LRAT), which catalyzes ROH esterification, was generated. Ectopic overexpression of either hSTRA6 or dSTRA6 in LRAT-expressing NIH 3T3 fibroblasts enhanced ROH uptake from holo-RBP to a similar extent, and introduction of TTR similarly decreased the rate of uptake (Fig. 2a and b). The similarity of the response of dSTRA6, which is unlikely to contain a TTR-binding capability, to that of hSTRA6 suggests that STRA6 in both species recognizes only free and not TTR-bound holo-RBP.

The question of whether STRA6 binds free or TTR-bound holo-RBP was then directly addressed. Recombinant holo-RBP was incubated alone or in the presence of TTR with the chemical cross-linker bis(sulfosuccinimidyl) suberate (0.5 mM, 14 h), resulting in efficient cross-linking of the holo-RBP-TTR complex (Fig. 2c). The mixtures and additional cross-linker were added to NIH 3T3 cells ectopically overexpressing histidine-tagged STRA6. STRA6 was immunoprecipitated, and precipitated proteins were resolved by SDS-PAGE and immunoblotted for RBP-containing complexes (Fig. 2d). Cross-linking of cells with holo-RBP resulted in the appearance of a band with a molecular mass of ~100 kDa, corresponding to that of an RBP-bound STRA6. No such band was observed in cells cross-linked with the RBP-ROH-TTR complex, and no bands that might correspond to a STRA6-RBP-TTR (~150 kDa) appeared. The data thus indicate that STRA6 associates only with free holo-RBP and that the presence of TTR prevents the association.

To further examine whether TTR inhibits STRA6-mediated

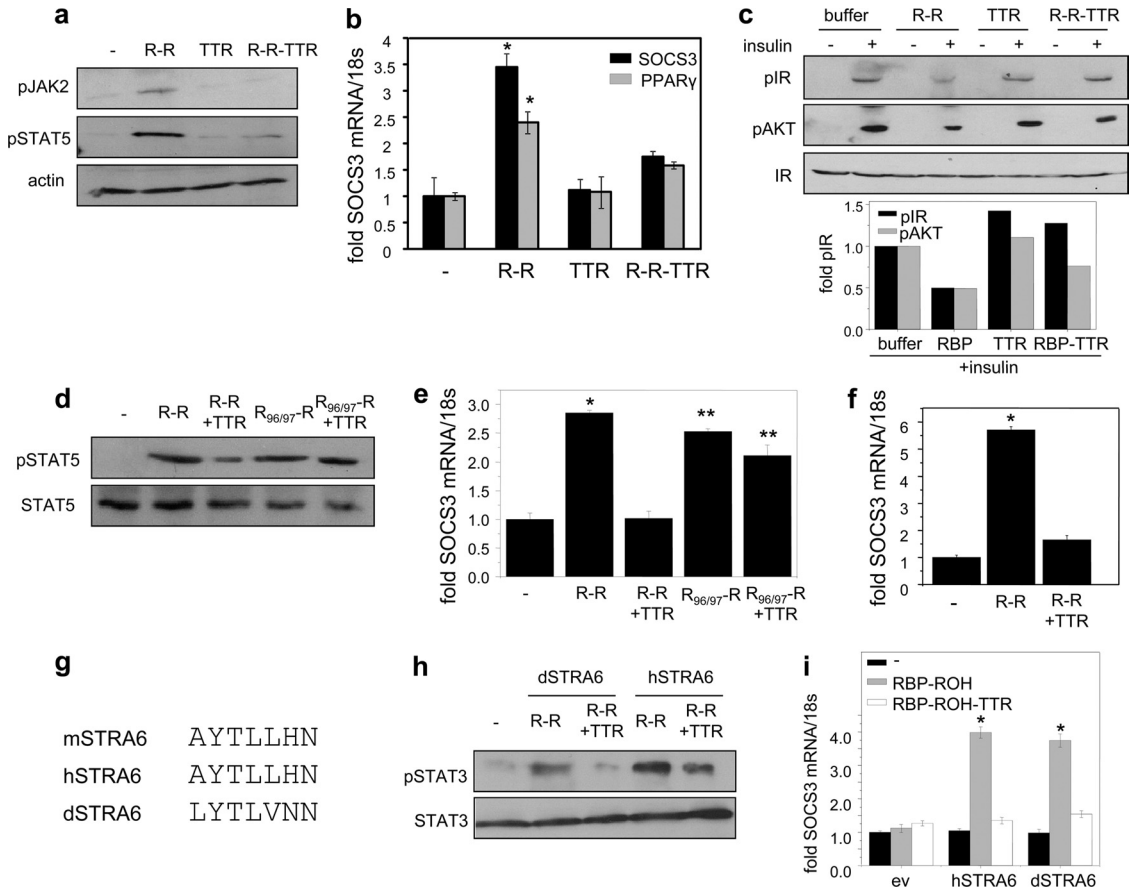

FIG 3 TTR blocks activation of STRA6 signaling by holo-RBP. (a) NIH 3T3-L1 adipocytes were treated with 1 μM RBP-ROH (R-R), TTR, or RBP-ROH-TTR (R-R-TTR) for 15 min. Cells were lysed, and phosphorylated JAK2 (pJAK2) and STAT5 (pSTAT5) were visualized by immunoblotting. (b) NIH 3T3-L1 adipocytes cells were treated with 1 μM RBP-ROH, TTR, or RBP-ROH-TTR for 4 h, and levels of SOCS3 and PPARγ mRNA were assessed by Q-PCR. Data are means ± SEM. *, $P < 0.001$ versus nontreated cells. (c) NIH 3T3-L1 adipocytes were pretreated with 1 μM RBP-ROH, TTR, or RBP-ROH-TTR for 8 h and then treated with insulin (25 nM, 15 min.). Phosphorylated IR (pIR) and AKT (pAKT) were visualized by immunoblotting. Bottom, quantitation of band intensities. Means of two independent experiments. (d) NIH 3T3-L1 adipocytes were treated with RBP-ROH or RBP-F96A/L97A-ROH ($RBP_{96/97}$-R) in the presence or absence of TTR (1 μM each, 15 min). Lysates were immunoblotted for pSTAT5. (e) NIH 3T3-L1 adipocytes were treated with RBP-ROH or RBP-F96A/L97A-ROH in the presence or absence of TTR (1 μM each, 4 h). Levels of SOCS3 mRNA were assessed by Q-PCR. Data are means ± SEM. *, $P < 0.001$ versus nontreated cells; **, $P < 0.001$ versus R-R-TTR-treated cells. (f) HepG2 cells were treated with RBP-ROH in the presence or absence of TTR (1 μM each, 4 h). Levels of SOCS3 mRNA were assessed by Q-PCR. Data are means ± SEM. *, $P < 0.001$ versus nontreated cells. (g) The phosphotyrosine motifs in mouse, human, and zebrafish STRA6 (mSTRA6, hSTRA6, and dSTRA6). (h) NIH 3T3 fibroblasts stably expressing LRAT were transfected with zebrafish and human STRA6 and treated with 1 μM RBP-ROH or RBP-ROH-TTR for 15 min, and lysates were immunoblotted for pSTAT3. (i) NIH 3T3 fibroblasts stably overexpressing LRAT were transfected with dSTRA6 or hSTRA6 and treated with 1 μM RBP-ROH or RBP-ROH-TTR for 4 h. Levels of SOCS3 mRNA were assessed by Q-PCR. Data are means ± SEM. *, $P < 0.001$ versus nontreated cells. All *P* values were calculated using a two-tailed student *t* test.

ROH uptake by preventing holo-RBP from binding to the receptor, an RBP mutant defective in its ability to bind TTR was generated. The reported three-dimensional crystal structure of the holo-RBP-TTR complex suggests that the interactions between the two proteins are mediated by several residues, including Phe96 and Leu97 (18). An RBP mutant in which these residues were replaced with alanines (RBP-F96A/L97A) was thus generated. The mutations did not alter the affinity of RBP for retinol (Fig. 2e), indicating that the overall fold of the mutant is intact. As expected, the F96A/L97A mutations disrupted the association of RBP with TTR (Fig. 2f). Measurements of ROH uptake showed that, in contrast with its inhibitory activity on ROH uptake from WT-RBP, TTR had no effect on ROH uptake from RBP-F96A/L97A (Fig. 2g). These observations further establish that TTR inhibits STRA6-mediated ROH uptake by sequestering holo-RBP and not by direct association with the receptor.

TTR inhibits holo-RBP-induced STRA6 signaling. The effect of TTR on RBP-induced STRA6 signaling was then examined using NIH 3T3-L1 adipocytes. We previously showed that in these cells, activation of STRA6 by holo-RBP triggers a JAK2/STAT5 cascade to induce the STAT target genes SOCS3 and PPARγ and inhibit insulin responses (2). Preadipocytes NIH 3T3-L1 cells were grown 2 days past confluence and induced to differentiate using a standard hormone mix (10 μg/ml insulin, 0.5 mM 3-isobutyl-1-methylxanthine [IBMX], 0.25 mM dexamethasone). Three days later, media were replaced and cells grown for 4 days. Differentiation was verified by monitoring lipid accumulation and by examining the expression of the adipocyte marker FABP4 (3). As expected, treatment of differentiated adipocytes with holo-RBP (R-R) increased the phosphorylation levels of JAK2 and STAT5 (Fig. 3a). In contrast, the holo-RBP-TTR complex did not alter the phosphorylation status of these proteins (Fig. 3a). Ac-

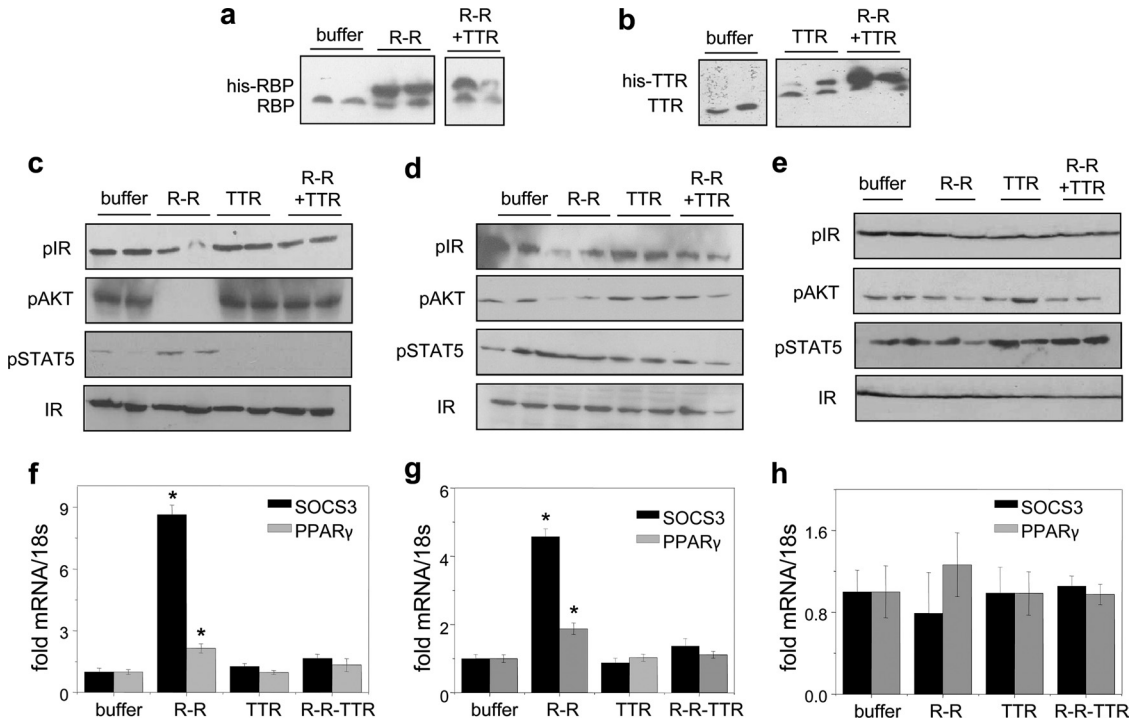

FIG 4 TTR suppresses activation of STRA6 by holo-RBP *in vivo*. Mice were injected three times with 0.1 μmol RBP-ROH or 0.1 μmol RBP-ROH complexed with TTR and sacrificed 1 h after the last injection. (a, b) Immunoblots of RBP (a) and TTR (b) in serum following the respective injections. Blots from 2 mice of each group are shown. (c to e) Immunoblots of phosphorylated insulin receptor (pIR), AKT (pAKT), and STAT5 (pSTAT5) in WAT (c), skeletal muscle (d), and liver (e) of mice treated as denoted. Total IR served as a loading control. (f to h) Levels of mRNA of SOCS3 and PPARγ in WAT (f), skeletal muscle (g), and liver (h) of treated mice. Data are means ± SEM. *, $P < 0.001$ for buffer-treated versus RBP-ROH-treated mice.

cordingly, TTR-bound holo-RBP failed to induce the expression of SOCS3 and PPARγ (Fig. 3b). To examine the effect of TTR on the ability of holo-RBP to suppress insulin responses, cells were pretreated with holo-RBP or holo-RBP-TTR for 8 h and treated with insulin for 15 min, and the levels of phosphorylation of the insulin receptor (IR) and its downstream effector AKT were monitored. The data show that inhibition of insulin-induced phosphorylation of IR and AKT by holo-RBP was blunted in the presence of TTR (Fig. 3c). TTR also inhibited the ability of holo-RBP, but not of holo-RBP-F96A/L97A, defective in TTR binding, to trigger STAT5 phosphorylation (Fig. 3d) or to induce the expression of SOCS3 in NIH 3T3-L1 adipocytes (Fig. 3e) or in HepG2 cells (Fig. 3f).

The effect of TTR on signaling by the zebrafish STRA6 was then examined. Notably, the phosphotyrosine in the cytosolic domain of STRA6, the STAT recruitment site of the receptor, is present in the dSTRA6, suggesting evolutionary conservation of STRA6 signaling (Fig. 3g). In these experiments, NIH 3T3 fibroblasts that ectopically overexpress LRAT were transfected with expression vectors for either hSTRA6 or dSTRA6. Treatment of cells expressing either hSTRA6 or dSTRA6 with holo-RBP induced phosphorylation of STAT3, the preferred STRA6-activated STAT in these cells (Fig. 3h), and upregulation of SOCS3 (Fig. 3i). TTR suppressed the ability of holo-RBP to induce STAT3 phosphorylation and to upregulate SOCS3 expression in cells expressing either hSTRA6 or dSTRA6 (Fig. 3h and i).

TTR inhibits the ability of holo-RBP to suppress insulin responses *in vivo*. The effect of TTR on the ability of holo-RBP to promote insulin resistance *in vivo* was then investigated. Eight-week-old mice were injected with recombinant holo-RBP, TTR, or holo-RBP-TTR. Mice were injected three times at 2-h intervals and sacrificed an hour after the last injection. The treatments resulted in respective elevation of serum levels of RBP, TTR, or both (Fig. 4a and b). As expected, treatment of mice with holo-RBP reduced the phosphorylation levels of the insulin receptor and AKT and induced the expression of SOCS3 and PPARγ in WAT (Fig. 4c and f) and skeletal muscle (Fig. 4d and g) but not in liver (Fig. 4e and h). In contrast, treatment with RBP-ROH-TTR did not affect the phosphorylation of IR and AKT or the expression levels of the STAT target genes (Fig. 4c to h).

The observations that only free and not TTR-bound holo-RBP activates STRA6 suggest that the serum RBP/TTR ratio is crucial for regulating STRA6 signaling. In agreement with the report that expression of RBP in adipose tissue increases in obese rodents and humans, resulting in elevation of serum RBP levels (35), feeding mice a high-fat, high-sucrose (HFHS) diet for 10 weeks resulted in upregulation of the expression of RBP in WAT but not in liver (Fig. 5a). In contrast, TTR expression in these organs was not affected by the diet (Fig. 5b). Accordingly, the serum level of RBP was markedly elevated, while the serum level of TTR remained unchanged in obese mice (Fig. 5c). Hence, the RBP/TTR ratio is significantly higher in blood of obese than of lean mice.

To directly determine if TTR prevents holo-RBP-induced insulin resistance, mice were treated with holo-RBP or holo-RBP-TTR for 3 weeks prior to the glucose tolerance tests (GTT). Mice were treated by implanting Alzet osmotic pumps containing the appropriate proteins (1 μM), thereby delivering constant amounts of proteins over the 3-week period. Similar to what was

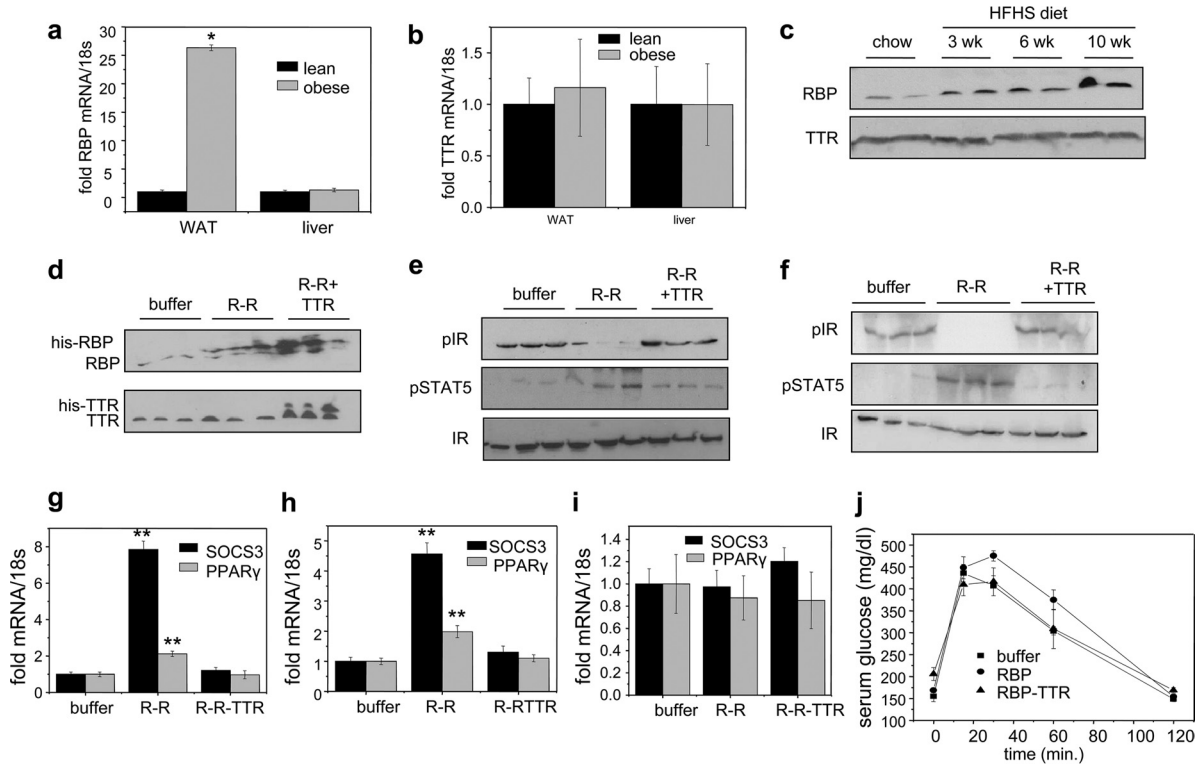

FIG 5 TTR is protective against holo-RBP-induced insulin resistance. (a and b) Levels of mRNA of RBP (a) and TTR (b) in WAT and liver of lean mice and of mice fed an HFHS diet for 10 weeks (obese). (c) Immunoblots of RBP and TTR in serum of mice fed an HFHS diet for 0, 3, 6, and 10 weeks. (d to j) Mice were implanted with an Alzet pump that contained buffer, 0.1 μM holo-RBP, or 0.1 μM holo-RBP complexed with TTR. Implants were replaced once a week for 3 weeks. (d) Immunoblots of RBP (top) and TTR (bottom) in serum following 3 weeks of denoted treatments. (e, f) Immunoblots of pIR and pSTAT5 in WAT (e) and skeletal muscle (f) of mice treated as denoted. (g to i) Levels of SOCS3 mRNA in WAT (g), skeletal muscle (h), and liver (i) of mice treated as denoted. (j) Glucose tolerance tests carried out following 3 weeks of denoted treatments. Data are means ± SEM. *, $P < 0.001$ for lean versus obese mice; **, $P < 0.001$ for buffer-treated versus RBP-ROH-treated mice. All *P* values were calculated using a two-tailed Student *t* test.

seen in the short-term treatments (Fig. 4), 3-week treatment of mice with holo-RBP induced phosphorylation of STAT5, reduced the activation level of IR, and upregulated SOCS3 and PPARγ in WAT (Fig. 5e and g) and muscle (Fig. 5f and h) but not in the liver (Fig. 5i). In contrast, treatment with TTR-bound holo-RBP had no effect on the phosphorylation of STAT5 or IR and did not alter the expression levels of the STAT target genes (Fig. 5e to i). Accordingly, while holo-RBP treatment resulted in a sluggish response in GTT, reflecting the development of insulin resistance, treatment with the holo-RBP-TTR complex did not alter the insulin responses of the mice (Fig. 5j). Hence, association with TTR suppresses the ability of holo-RBP to interfere with insulin signaling.

DISCUSSION

Upon binding of extracellular holo-RBP, STRA6 transports ROH into cells, and it activates a signaling cascade culminating in induction of STAT target genes (4, 5). The observations described here reveal that the binding partner of RBP in blood, TTR, effectively blocks association of holo-RBP with STRA6. Consequently, STRA6 mediates cellular ROH uptake only from free and not from TTR-bound holo-RBP. The data further show that, even in the presence of free holo-RBP, STRA6-mediated ROH uptake by tissues comprises only a small fraction of total uptake by target tissues *in vivo* (Fig. 1h). The observations thus support the previously proposed model whereby supply of ROH from circulating holo-RBP or holo-RBP-TTR to cells occurs primarily by diffusion through the plasma membranes (10, 14, 20, 21). Taken together with the observations that ROH transport by STRA6 is critical for enabling activation of STRA6 signaling (5), the data indicate that, with the exception of the eye (26), the main role of ROH transport by STRA6 is not to provide the vitamin to cells but to couple sensing of circulating free holo-ROH levels to cell signaling. It is worth noting that even in the eye, morphological changes and reduction in visual function in *Stra6*-null mice are mild, indicating that STRA6 is not the only pathway by which ROH enters the retinal pigment epithelium (26).

The data reveal that, in addition to its function in preventing filtration of the 21-kDa RBP in the kidney, TTR plays an important role in protecting cells from holo-RBP-induced signaling mediated by STRA6. The observations that STRA6 "senses" only free and not TTR-bound RBP establish that the receptor functions only under circumstances in which the serum RBP level exceeds that of TTR. Such circumstances are encountered, for example, in obese animals in which the serum level of RBP is elevated while the TTR level is not (Fig. 5c). The circumstances under which the plasma RBP concentration exceeds that of TTR in healthy lean animals remain to be clarified. In this regard, it is interesting that it has long been known that insulin responsiveness varies in a circadian fashion (17, 31). The molecular basis for these diurnal

variations is incompletely understood, but the data presented here raise the intriguing possibility that they may arise from diurnal variations in the plasma RBP/TTR ratio.

The RBP/TTR ratio in blood may be altered by changes in the expression level of RBP, or TTR, or both. TTR is expressed in the central nervous system and in the liver, with the latter serving as the main source for the protein in serum (9). Expression of hepatic TTR is downregulated, and consequently, the serum TTR level dramatically decreases during the acute-phase response (APR), a process characterized by rapid reprogramming of gene expression and metabolism in response to inflammatory cytokine signaling (1, 22). The low serum level of TTR associated with APR may release holo-RBP, thereby activating STRA6. Hence, STRA6 signaling may play a role in APR. It has also been reported that hepatic TTR expression is regulated by sex hormones (12) and is directly controlled by hepatocyte nuclear factor 4α (HNF-4α) (30). The expression of RBP in brown adipose tissue and liver was reported to be regulated by cyclic AMP-mediated pathways and by the nuclear receptors PPARα and PPARγ (6, 25). Whether, by controlling TTR or RBP expression, these factors regulate the RBP-TTR ratio in blood and thus STRA6 signaling remains to be clarified.

Notably, as free holo-RBP is rapidly excreted by glomerular filtration, its lifetime in serum is short. Holo-RBP thus functions like a classical cytokine: its availability to its membrane receptor is tightly regulated, and its signaling activities are constrained by a short half-life in the circulation. These characteristics of the signaling activities of holo-RBP strikingly differ from the characteristics of its role as a shuttling protein that mobilizes ROH from liver stores. Unlike in the former capacity, where holo-RBP functions on its own, delivery of ROH to target tissues is mediated by the holo-RBP-TTR complex. The plasma level of this complex is under tight homeostatic control, and it provides ROH to target cells to support tissue requirement for vitamin A without the need for a specialized receptor.

ACKNOWLEDGMENTS

We are grateful to Michele Mumaw for help in early stages of this work. We thank Lawreen Connors, Boston University School of Medicine, and Silke Vogel, Columbia University School of Physicians and Surgeons, for the TTR and RBP expression constructs.

This work was supported by NIH grants DK060684 and CA107013 to N.N. The Mouse Metabolic Phenotyping Center of Case Western Reserve University is supported by NIH grant DK59630. The *Stra6*-null mouse line was established at the Mouse Clinical Institute (http://www-mci.u-strasbg.fr/) in the Genetic Engineering and Model Validation Department with INSERM and FRM (DEQ20071210544) grants to N.B.G.

REFERENCES

1. **Baumann H, Gauldie J.** 1994. The acute phase response. Immunol. Today **15**:74–80.
2. **Berry DC, Jin H, Majumdar A, Noy N.** 2011. Signaling by vitamin A and retinol-binding protein regulates gene expression to inhibit insulin responses. Proc. Natl. Acad. Sci. U. S. A. **108**:4340–4345.
3. **Berry DC, Noy N.** 2009. All-trans-retinoic acid represses obesity and insulin resistance by activating both peroxisome proliferation-activated receptor beta/delta and retinoic acid receptor. Mol. Cell. Biol. **29**:3286–3296.
4. **Berry DC, Noy N.** 2012. Signaling by vitamin A and retinol-binding protein in regulation of insulin responses and lipid homeostasis. Biochim. Biophys. Acta **1821**:168–176.
5. **Berry DC, O'Byrne SM, Vreeland AC, Blaner WS, Noy N.** 2012. Cross talk between signaling and vitamin A transport by the retinol-binding protein receptor STRA6. Mol. Cell. Biol. **32**:3164–3175.
6. **Bianconcini A, et al.** 2009. Transcriptional activity of the murine retinol-binding protein gene is regulated by a multiprotein complex containing HMGA1, p54 nrb/NonO, protein-associated splicing factor (PSF) and steroidogenic factor 1 (SF1)/liver receptor homologue 1 (LRH-1). Int. J. Biochem. Cell Biol. **41**:2189–2203.
7. **Cogan U, Kopelman M, Mokady S, Shinitzky M.** 1976. Binding affinities of retinol and related compounds to retinol binding proteins. Eur. J. Biochem. **65**:71–78.
8. **Croker BA, Kiu H, Nicholson SE.** 2008. SOCS regulation of the JAK/STAT signalling pathway. Semin. Cell Dev. Biol. **19**:414–422.
9. **Felding P, Fex G.** 1982. Cellular origin of prealbumin in the rat. Biochim. Biophys. Acta **716**:446–449.
10. **Fex G, Johannesson G.** 1988. Retinol transfer across and between phospholipid bilayer membranes. Biochim. Biophys. Acta **944**:249–255.
11. **Germain P, et al.** 2006. International Union of Pharmacology. LX. Retinoic acid receptors. Pharmacol. Rev. **58**:712–725.
12. **Goncalves I, et al.** 2008. Transthyretin is up-regulated by sex hormones in mice liver. Mol. Cell. Biochem. **317**:137–142.
13. **Heller J.** 1975. Interactions of plasma retinol-binding protein with its receptor. Specific binding of bovine and human retinol-binding protein to pigment epithelium cells from bovine eyes. J. Biol. Chem. **250**:3613–3619.
14. **Hodam JR, Creek KE.** 1998. Comparison of the metabolism of retinol delivered to human keratinocytes either bound to serum retinol-binding protein or added directly to the culture medium. Exp. Cell Res. **238**:257–264.
15. **Kawaguchi R, et al.** 2007. A membrane receptor for retinol binding protein mediates cellular uptake of vitamin A. Science **315**:820–825.
16. **Kingsbury JS, Klimtchuk ES, Theberge R, Costello CE, Connors LH.** 2007. Expression, purification, and in vitro cysteine-10 modification of native sequence recombinant human transthyretin. Protein Expr. Purif. **53**:370–377.
17. **Lee A, Ader M, Bray GA, Bergman RN.** 1992. Diurnal variation in glucose tolerance. Cyclic suppression of insulin action and insulin secretion in normal-weight, but not obese, subjects. Diabetes **41**:750–759.
18. **Naylor HM, Newcomer ME.** 1999. The structure of human retinol-binding protein (RBP) with its carrier protein transthyretin reveals an interaction with the carboxy terminus of RBP. Biochemistry **38**:2647–2653.
19. **Norris AW, Li E.** 1998. Fluorometric titration of the CRABPs. Methods Mol. Biol. **89**:123–139.
20. **Noy N, Xu ZJ.** 1990. Interactions of retinol with binding proteins: implications for the mechanism of uptake by cells. Biochemistry **29**:3878–3883.
21. **Noy N, Xu ZJ.** 1990. Kinetic parameters of the interactions of retinol with lipid bilayers. Biochemistry **29**:3883–3888.
22. **Pepys MB, Baltz ML.** 1983. Acute phase proteins with special reference to C-reactive protein and related proteins (pentaxins) and serum amyloid A protein. Adv. Immunol. **34**:141–212.
23. **Prapunpoj P.** 2009. Evolutionary changes to transthyretin. FEBS J. **276**:5329. doi:10.1111/j.1742-4658.2009.07242.x.
24. **Raz A, Goodman DS.** 1969. The interaction of thyroxine with human plasma prealbumin and with the prealbumin-retinol-binding protein complex. J. Biol. Chem. **244**:3230–3237.
25. **Rosell M, et al.** 2012. Peroxisome proliferator-activated receptors-alpha and -gamma, and cAMP-mediated pathways, control retinol-binding protein-4 gene expression in brown adipose tissue. Endocrinology **153**:1162–1173.
26. **Ruiz A, et al.** 2012. Retinoid content, visual responses and ocular morphology are compromised in the retinas of mice lacking the retinol-binding protein receptor, STRA6. Invest. Ophthalmol. Vis. Sci. **53**:3027–3039.
27. **Schug TT, Berry DC, Shaw NS, Travis SN, Noy N.** 2007. Opposing effects of retinoic acid on cell growth result from alternate activation of two different nuclear receptors. Cell **129**:723–733.
28. **Shingleton JL, Skinner MK, Ong DE.** 1989. Characteristics of retinol accumulation from serum retinol-binding protein by cultured Sertoli cells. Biochemistry **28**:9641–9647.
29. **Wald G.** 1968. The molecular basis of visual excitation. Nature **219**:800–807.
30. **Wang Z, Burke PA.** 2010. Hepatocyte nuclear factor-4alpha interacts with other hepatocyte nuclear factors in regulating transthyretin gene expression. FEBS J. **277**:4066–4075.

31. **Whichelow MJ, et al.** 1974. Diurnal variation in response to intravenous glucose. Br. Med. J. **i**:488–491.
32. **Wilson JG, Roth CB, Warkany J.** 1953. An analysis of the syndrome of malformations induced by maternal vitamin A deficiency. Effects of restoration of vitamin A at various times during gestation. Am. J. Anat. **92**:189–217.
33. **Wolbach SB, Howe PR.** 1978. Nutrition classics. The Journal of Experimental Medicine 42:753–77, 1925. Tissue changes following deprivation of fat-soluble A vitamin. S. Burt Wolbach and Percy R. Howe. Nutr. Rev. **36**:16–19.
34. **Xie Y, Lashuel HA, Miroy GJ, Dikler S, Kelly JW.** 1998. Recombinant human retinol-binding protein refolding, native disulfide formation, and characterization. Protein Expr. Purif. **14**:31–37.
35. **Yang Q, et al.** 2005. Serum retinol binding protein 4 contributes to insulin resistance in obesity and type 2 diabetes. Nature **436**:356–362.